

AD-A132 104

ASYMPTOTIC HIGH FREQUENCY TECHNIQUES FOR UHF AND ABOVE
ANTENNAS(U) OHIO STATE UNIV COLUMBUS ELECTROSCIENCE LAB
W D BURNSIDE ET AL. NOV 77 ESL-4508-7 N00123-76-C-1371

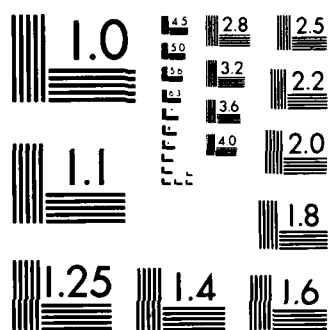
1/1

UNCLASSIFIED

F/G 9/5

NL





MICROCOPY RESOLUTION TEST CHART
NATIONAL BUREAU OF STANDARDS 1963 A



ASYMPTOTIC HIGH FREQUENCY TECHNIQUES FOR UHF AND ABOVE ANTENNAS

Fifth Quarterly Report - 1 August to 31 October 1977

W.D. Burnside
R.J. Marhefka
R.C. Rudduck
C.H. Walter

The Ohio State University

ElectroScience Laboratory

Department of Electrical Engineering
Columbus, Ohio 43212

Quarterly Report 4508-7 (784508)

1 August to 31 October 1977

November 1977

Contract N00123-76-C-1371

Approved for public release;
distribution unlimited.

DTIC
ELECTE
SEP 06 1983
S D E

Naval Regional Procurement Office
Long Beach, California 90822

83 08 29 048

~~82 10 12 015~~

ADA 132107

DTIC FILE COPY

NOTICES

When Government drawings, specifications, or other data are used for any purpose other than in connection with a definitely related Government procurement operation, the United States Government thereby incurs no responsibility nor any obligation whatsoever, and the fact that the Government may have formulated, furnished, or in any way supplied the said drawings, specifications, or other data, is not to be regarded by implication or otherwise as in any manner licensing the holder or any other person or corporation, or conveying any rights or permission to manufacture, use, or sell any patented invention that may in any way be related thereto.

UNCLASSIFIED

SECURITY CLASSIFICATION OF THIS PAGE (When Data Entered)

REPORT DOCUMENTATION PAGE		READ INSTRUCTIONS BEFORE COMPLETING FORM
1. REPORT NUMBER	2. GOVT ACCESSION NO.	3. RECIPIENT'S CATALOG NUMBER
	AD-A137184	
4. TITLE (and Subtitle)		5. TYPE OF REPORT & PERIOD COVERED
ASYMPTOTIC HIGH FREQUENCY TECHNIQUES FOR UHF AND ABOVE ANTENNAS		Fifth Quarterly Report 1 August to 31 October 1977
7. AUTHOR(s)		6. PERFORMING ORG. REPORT NUMBER
W.D. Burnside, R.J. Marhefka, R.C. Rudduck, C.H. Walter		ESL 4508-7 (784508)
9. PERFORMING ORGANIZATION NAME AND ADDRESS		8. CONTRACT OR GRANT NUMBER(s)
The Ohio State University ElectroScience Laboratory, Department of Electrical Engineering, Columbus, Ohio 43212		N00123-76-C-1371
11. CONTROLLING OFFICE NAME AND ADDRESS		10. PROGRAM ELEMENT, PROJECT, TASK AREA & WORK UNIT NUMBERS
Naval Regional Procurement Office Long Beach, California 90822		Project N00953/6/009121
14. MONITORING AGENCY NAME & ADDRESS (if different from Controlling Office)		12. REPORT DATE
		November 1977
		13. NUMBER OF PAGES
		28
		15. SECURITY CLASS. (of this report)
		Unclassified
		15a. DECLASSIFICATION DOWNGRADING SCHEDULE
16. DISTRIBUTION STATEMENT (of this Report)		
Approved for public release; distribution unlimited.		
17. DISTRIBUTION STATEMENT (of the abstract entered in Block 20, if different from Report)		
18. SUPPLEMENTARY NOTES		
19. KEY WORDS (Continue on reverse side if necessary and identify by block number)		
Computer code Reflector Antenna Algorithm Aperture Integration Geometrical Theory of Diffraction Cylinders Far Field Pattern		
20. ABSTRACT (Continue on reverse side if necessary and identify by block number)		
The overall scope of the program on Contract No. N00123-76-C-1371 between The Ohio State University ElectroScience Laboratory and the Naval Electronics Laboratory Center is to develop the necessary theory, algorithms and computer codes for simulating antennas at UHF and above in a complex ship environment. The work consists of a) basic scattering code development, b) reflector antenna code development and c) basic studies to support items a) and b). This report describes the progress in each of these three areas for the period 1 August to 31 October 1977.		

DD FORM 1 JAN 73 1473

EDITION OF 1 NOV 65 IS OBSOLETE

UNCLASSIFIED

SECURITY CLASSIFICATION OF THIS PAGE (When Data Entered)

CONTENTS

	Page
I. INTRODUCTION	1
II. PROGRAM SCOPE	1
III. BASIC SCATTERING CODE DEVELOPMENT	5
IV. REFLECTOR ANTENNA CODE DEVELOPMENT	16
A. Feed Pattern	16
B. Rotating Grid Method	22
C. GTD Method	23
V. THEORETICAL STUDIES	26
REFERENCES	27

Accession For	
NTIS GRA&I	<input checked="" type="checkbox"/>
DTIC TAB	<input type="checkbox"/>
Unannounced	<input type="checkbox"/>
Justification	
By	
Distribution /	
Availability Codes	
Distribution /or	
Dist	
A	

COPY
INSPECTED
2

I. INTRODUCTION

This report describes the work done on Contract No. N00123-76-C-1371 for the period 1 August 1977 to 31 October 1977.

The overall program is divided into three areas. These are 1) basic scattering code development, 2) reflector antenna code development and 3) basic theoretical studies to support the first two areas. The following sections describe the research accomplished in each of the three areas mentioned above.

II. PROGRAM SCOPE

The scope of the work under Contract No. N00123-76-C-1371 is to develop the necessary theory, algorithms and computer codes for simulating antennas at UHF and above in a complex ship environment. A revised milestone chart for the three year program is shown in Table I. The milestone chart is revised from that shown in the Annual Report 1 August 1976 to 31 July 1977. These revisions were agreed upon at a project review meeting at NOSC as discussed below.

Project Review Meeting

A project review meeting was held on 5 October 1977 at NOSC with C.H. Walter, R.C. Rudduck, and W.D. Burnside representing Ohio State and J.W. Rockway, J. Logan, and S.T. Li representing NOSC. In this meeting the current status of the computer codes was described in detail. Computed results were shown to illustrate the powerful features of both the Basic Scattering Code and the Reflector Antenna Code. Both codes have great potential for solving electromagnetic interference problems in shipboard antenna systems. Furthermore, the codes can be used to predict the performance of future shipboard antenna designs.

At the project review meeting the planned deliverables and their projected completion dates were discussed. It was agreed to make some revisions in the deliverables which will not significantly change the capability of the codes and their documentation.

The major result of the revisions is that all deliverable items will be completed by the end of the third year. This was made possible by including the documentation for the computer codes in only two code manuals instead of four separate manuals.

At the request of Dr. Rockway several command features will be added to the delivered codes. The far field scattering code will include an option for range dependence. The reflector antenna code will include the capability to change the reflector geometry or the feed pattern independently so that data inputs can be substantially reduced in some cases. Furthermore, specific examples of Navy reflector antennas will be included in the user's manual. The planned deliverables and their projected completion dates are shown in Table II.

TABLE I. Revised Milestone Chart (10/05/77)

TABLE II - PLANNED DELIVERABLES

BASIC SCATTERING CODE DELIVERABLES

Projected Completion Date	<u>Flat Plates, Box and Cylinder (Independent)</u>
October 31, 1977	Computer Program Package (Delivered Oct. 5, 1977)
November 30, 1977	User Manual (Typed Rough Draft)
	<u>Coupled Solution For Flat Plates, Box and Cylinder*</u>
October 31, 1978	Computer Program Package
October 31, 1978	User Manual
March 31, 1979	Rough Draft of Code Manual
July 31, 1979	Code Manual

* Will supercede previous code

REFLECTOR ANTENNA CODE DELIVERABLES

Completion Date

Far Field Code

January 31, 1978

Computer Program Package

February 28, 1978

User Manual (Typed Rough Draft)

Near Field Code

October 31, 1978

Computer Program Package

October 31, 1978

User Manual

Code with Scattering from Feed and Supports**

April 30, 1979

Rough Draft of Code Manual

July 31, 1979

Code Manual

July 31, 1979

Computer Program Package

July 31, 1979

User Manual

** Will supercede previous two codes

III. BASIC SCATTERING CODE DEVELOPMENT

The purpose of this section is to describe the present status of the basic scattering code development program for the analysis of antennas in a complex shipboard environment. The Geometrical Theory of Diffraction (GTD) is being used to develop algorithms to solve for the scattering from basic plate and cylinder structures. These simple components can then be combined to form box-like structures with a nearby finite elliptic cylinder that can represent the various component structures of a ship. The algorithms are being implemented into a user-oriented computer code.

In this period, the NEC code has been interfaced with the GTD scattering code. The GTD code will accept as input data the output data of the NEC code which describes wire segment location, orientation, and excitation. The GTD code is written at present to use only the wire segment capabilities of the NEC code and not the patch segments. In order to simplify the interfacing of the two codes and to make the GTD code as fast and efficient as possible, the NEC currents are assumed to be the value of the current at the center of a segment with a cosine current distribution. This, of course, is not the same distribution as used in the NEC code but as is well known the radiation pattern is insensitive to the current distribution for segments shorter than $\lambda/4$. The GTD code is normalized in the far field to $\exp(-jkR)/R$. The fields are output in volts/meter, however, it should be noted that unless a range R is defined the units are actually in volts. The directive gain is also calculated by using the power radiated as supplied by the NEC code.

The interfacing of the NEC and GTD codes has been tested by using two examples obtained from Mr. Jim Logan at NOSC. Both examples are composed of antennas that were modeled by wire segments over a perfectly conducting infinite ground plane. Using the assumption that the current distributions obtained in this way will not be perturbed appreciably by slightly changing the environment, the currents from the NEC code can be used to simulate the radiation pattern for the antennas mounted over a finite plate which is over an infinite ground plane as shown in Figure 1.

To test the compatibility of the current distribution used in the GTD code with the current weights obtained from the NEC code, the GTD code was used to calculate the field for the example problem of four quarter-wavelength dipoles. The locations of the four dipoles are illustrated in Figure 1 as the four solid lines parallel to the x-axis. The infinite ground plane is coincident with the square plate for this first test. The dipoles were divided into a total of 20 segments. The fields obtained from this calculation should have exactly duplicated the fields as calculated by the NEC code. However, it was found that the GTD code was low by a factor of approximately 1.55. This is very close to a factor of one-half π which indicated the GTD code's cosine current distribution does not give the correct level when used for a

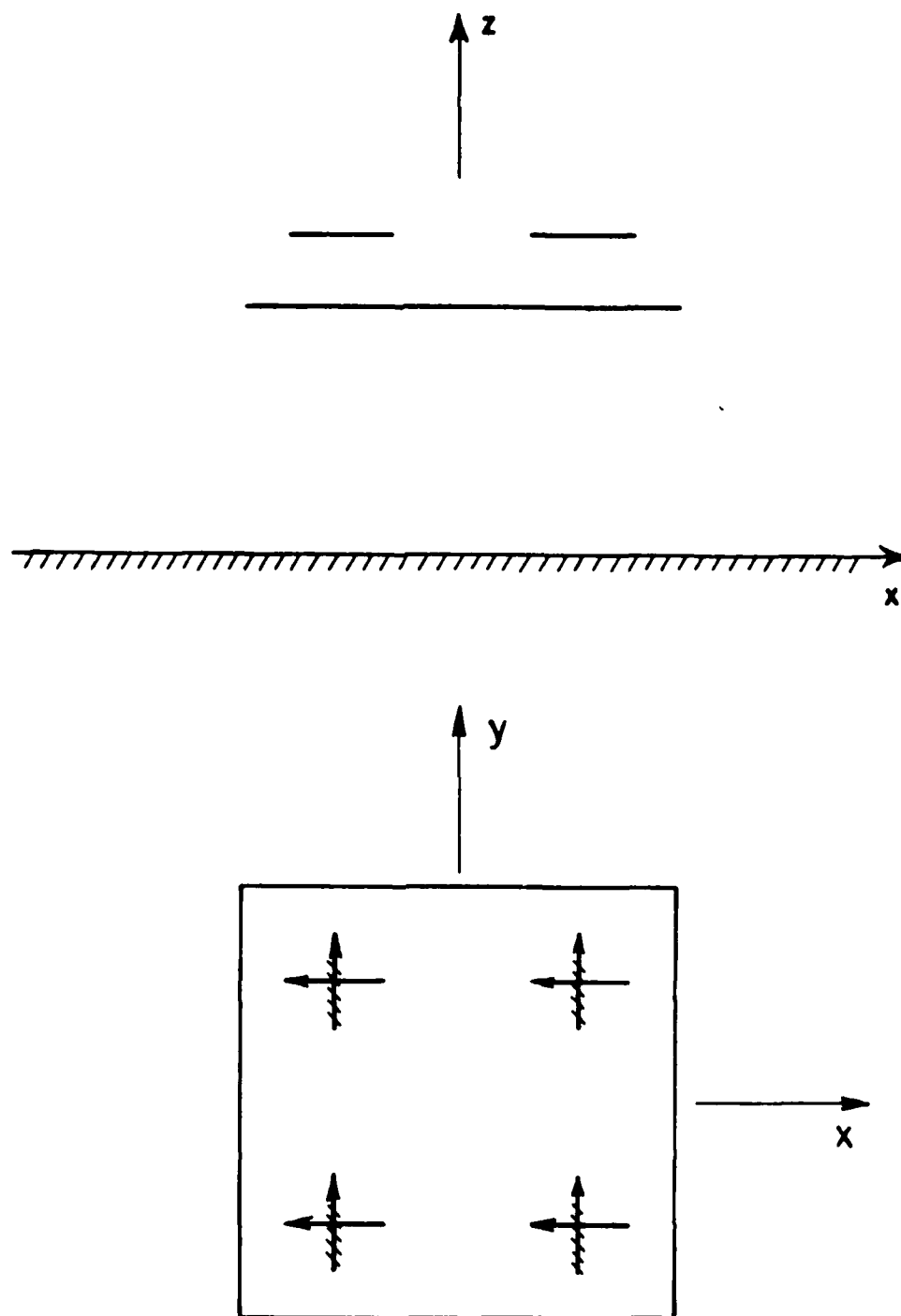


Figure 1. Geometry for the problems of dipoles over a square plate and infinite ground plane showing the side and top views.

small segment size. The pattern shapes for the two results, however, are identical. When a factor of one-half π was added to the GTD results the directive gains were within 0.2 dB as shown in Figures 2a and 2b for the plane $\phi=0^\circ$ and $\phi=90^\circ$, respectively. It should be noted that when the four quarter-wavelength dipoles with a cosine distribution weighted to the center current value is used directly in the GTD code, the field is very close to the NEC result and therefore does not need the factor of one-half π . The current distribution used in the GTD code, therefore, is only off for small sized segments. The factor of one-half π has been included in the code only when the NEC option is used and should be valid if the segment lengths used are on the order of approximately 0.1 wavelength or less.

The GTD code was next used to show how the directive gain changes when the four dipoles are placed over a square plate over a ground plane as shown in Figure 1. The comparisons between the infinite ground plane and square plate cases are shown in Figures 3a and 3b for the two pattern planes.

In order to confirm the above conclusions on the current distributions, a second example was used. This one is composed of four sets of crossed dipoles as shown in Figure 1 where solid and a dashed lines are used to represent the crossed dipoles. The results obtained from NOSC for this example were obtained from an AMP code print out rather than a NEC code print out; however, the results are still useful for comparison purposes. The GTD and AMP results for 48 segment dipoles over an infinite ground plane are compared in Figures 4a and 4b, where Figure 4a shows the vertical component and Figure 4b the horizontal component. The solid curves represent the GTD code with a factor of one-half π added and the X's show the AMP result. Again the two results compare within 0.2 dB. Square plate results are also shown in Figures 4a and 4b. Directive gains for the infinite ground plane and square plate cases are compared in Figures 5a and 5b for the $\phi=0^\circ$ and $\phi=45^\circ$ planes, respectively.

The second example confirms the conclusion of the first example that the GTD code and NEC code appear now to be properly interfaced. It should be noted that the directive gain is being computed using the power radiated as given in the NEC code. If this value is off in the NEC code then the GTD directive gain will be off by the same factor with everything else being the same. An alternative method of computing the directive gain would be to integrate the volumetric pattern of the GTD code and use that as the power radiated. This is possible but would not be an efficient method since it would be very costly to compute all the needed pattern values. This is especially true for the NEC code interface, since in general a large number of current segments will be used which increases the computer time needed for each pattern.

The basic scattering code that allows simulation of concave and convex plate structures and a finite elliptic cylinder structure without coupling between the plates and cylinder was completed and delivered to NOSC on 5 October 1977. The NEC code was interfaced in this code,

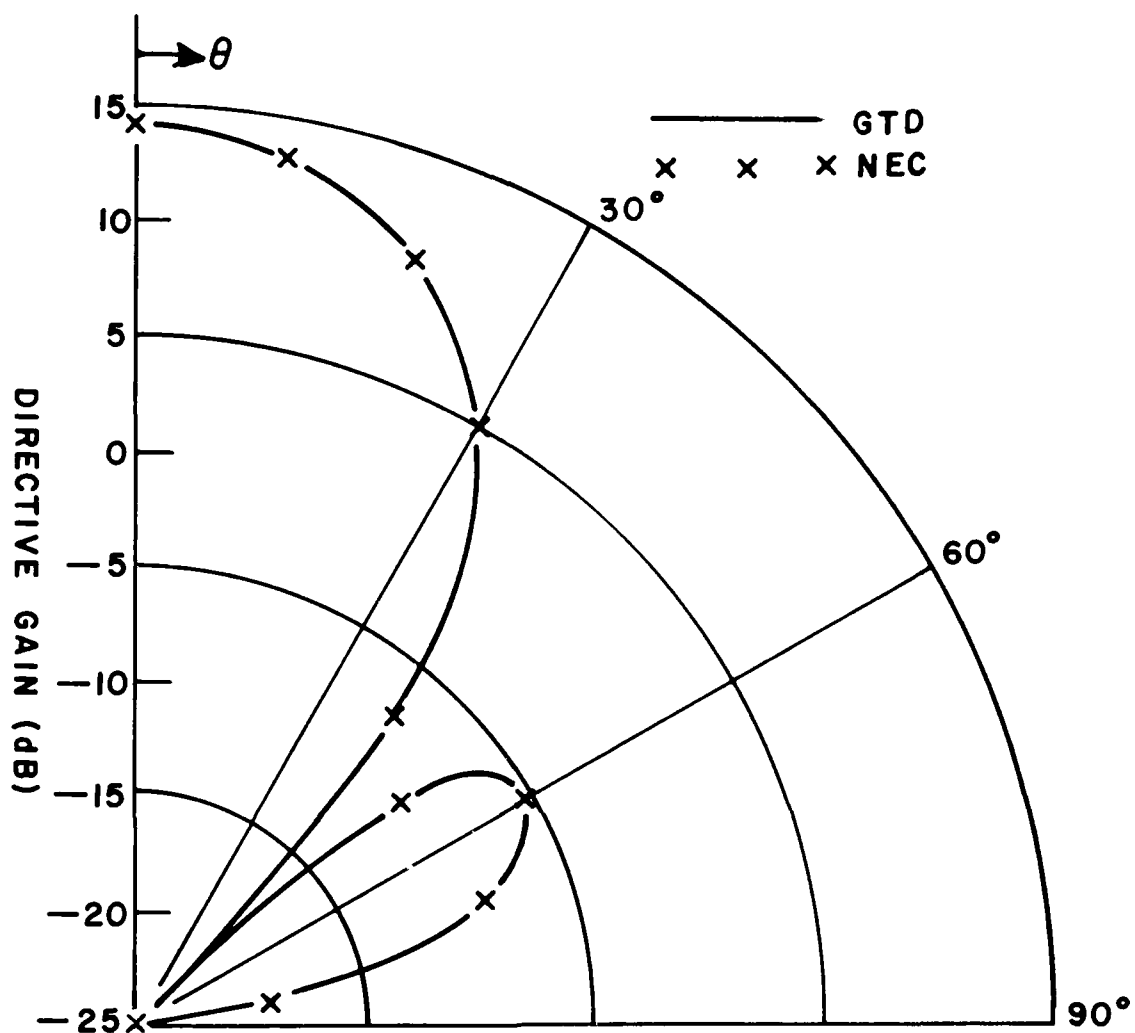


Figure 2a. Comparison of the directive gain of four dipoles over an infinite ground plane obtained from the NEC code and from the GTD code using the NEC currents ($\phi=0^\circ$ vertical polarization).

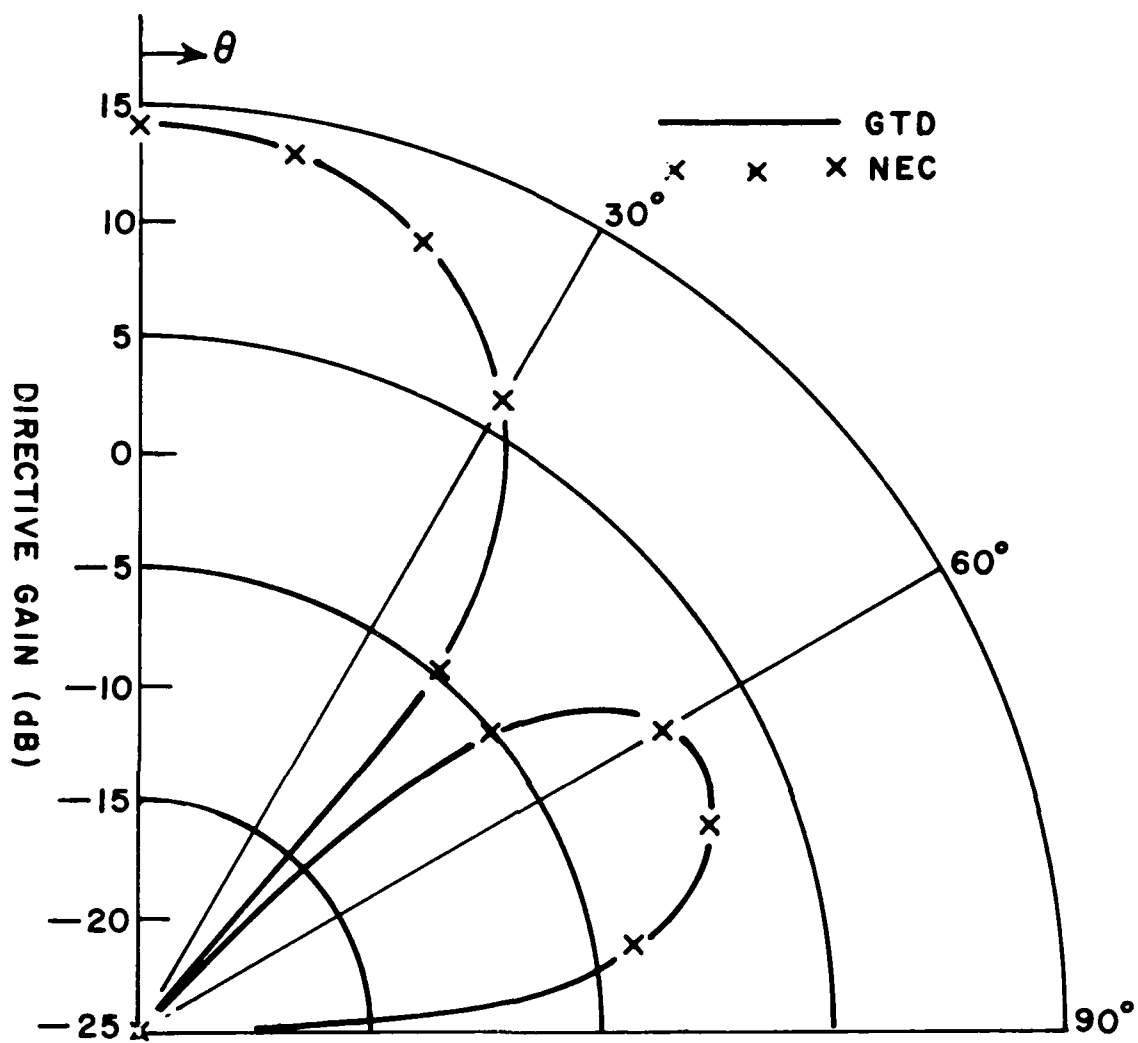


Figure 2b. Comparison of the directive gain of four dipoles over an infinite ground plane obtained from the NEC code and from the GTD code using the NEC currents ($\phi=90^\circ$ horizontal polarization).

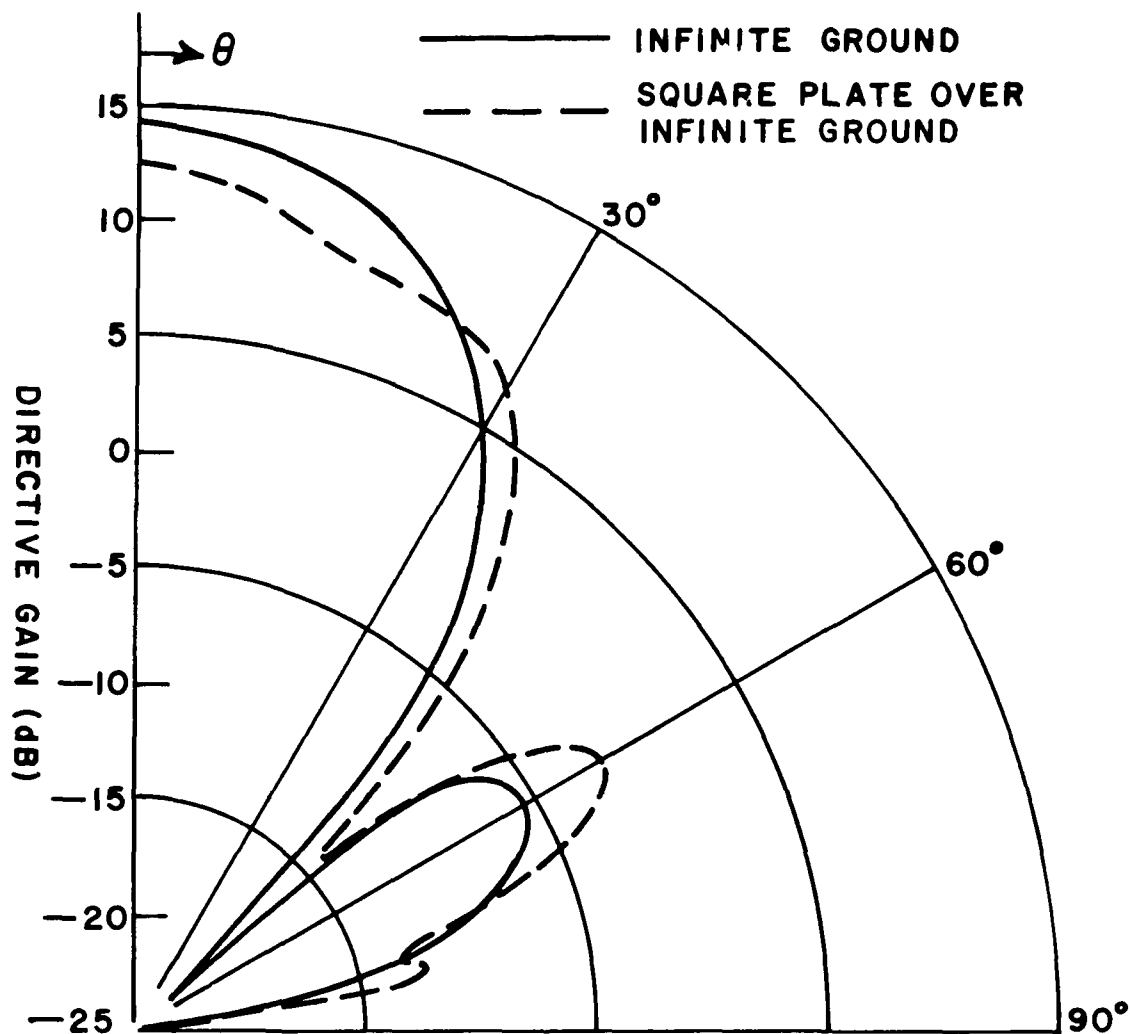


Figure 3a. Comparison of the directive gain of four dipoles over an infinite ground with four dipoles over a square plate over an infinite ground plane ($\phi=0^\circ$, vertical polarization).

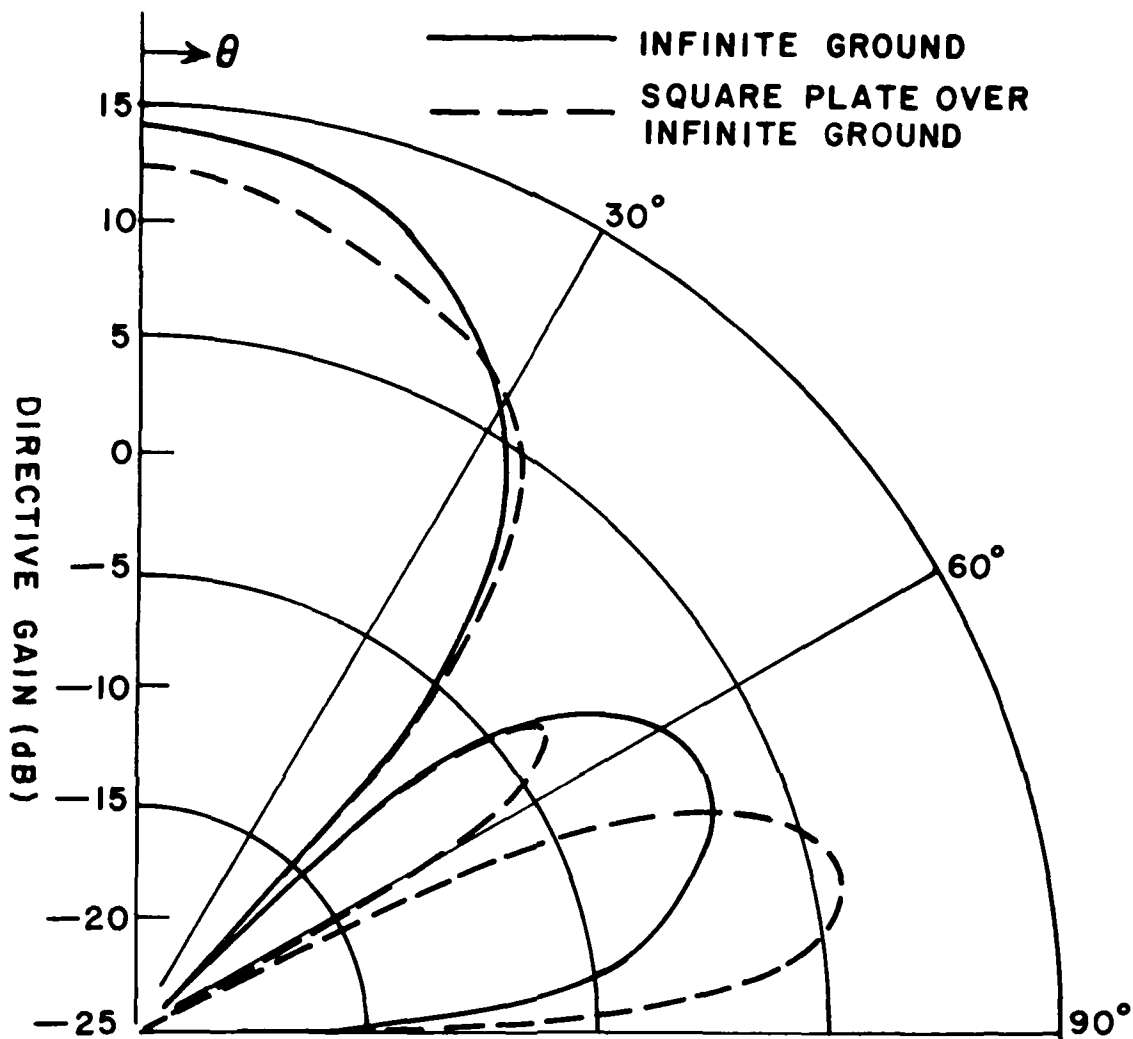


Figure 3b. Comparison of the directive gain of four dipoles over an infinite ground with four dipoles over a square plate over an infinite ground plane ($\phi=90^\circ$, horizontal polarization).

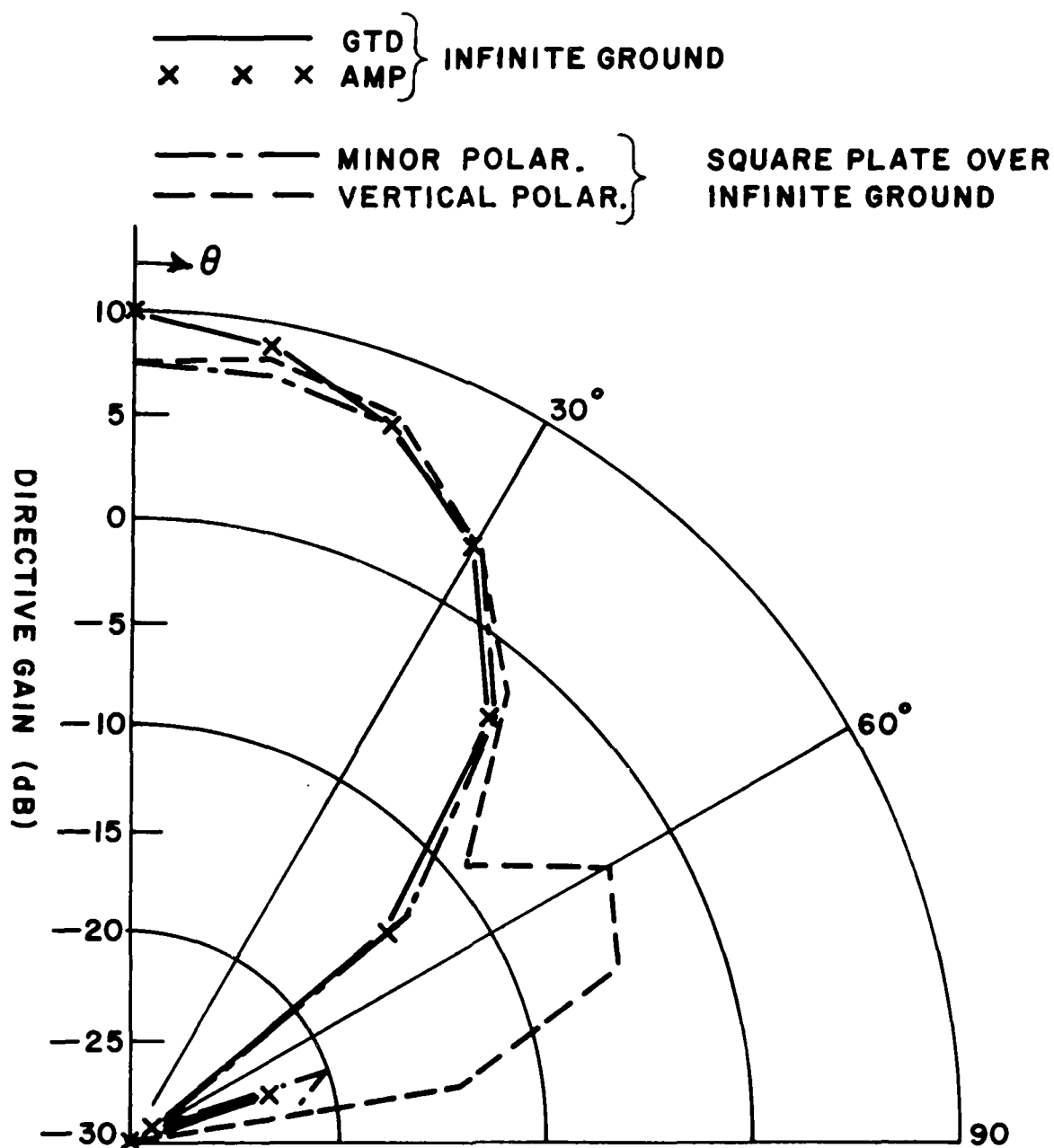


Figure 4a. Comparison of the directive gain of four sets of crossed dipoles over an infinite ground and over a square plate over an infinite ground ($\phi=0^\circ$, vertical polarization).

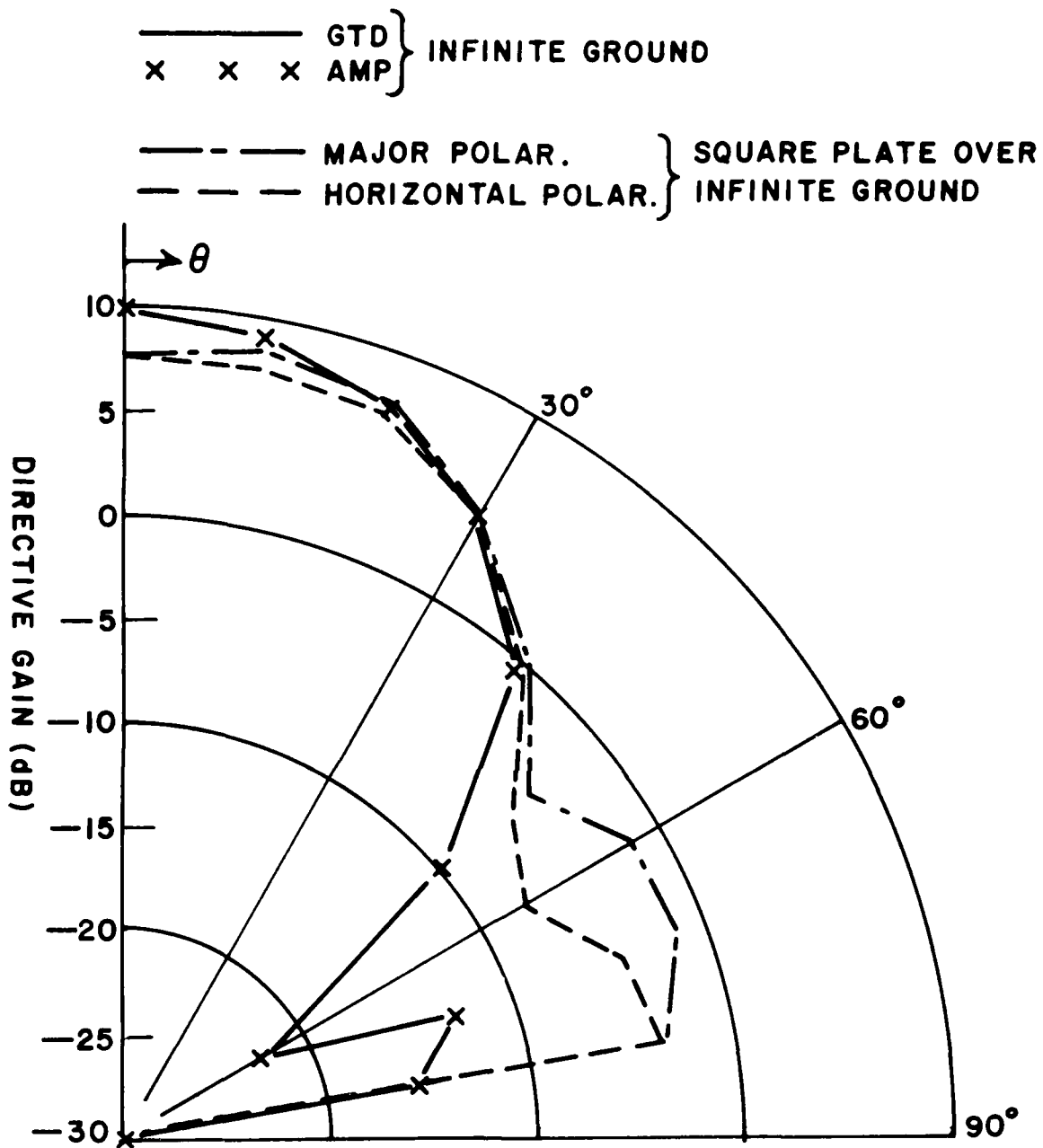


Figure 4b. Comparison of the directive gain of four sets of crossed dipoles over an infinite ground and over a square plate over an infinite ground ($\phi=0^\circ$, horizontal polarization).

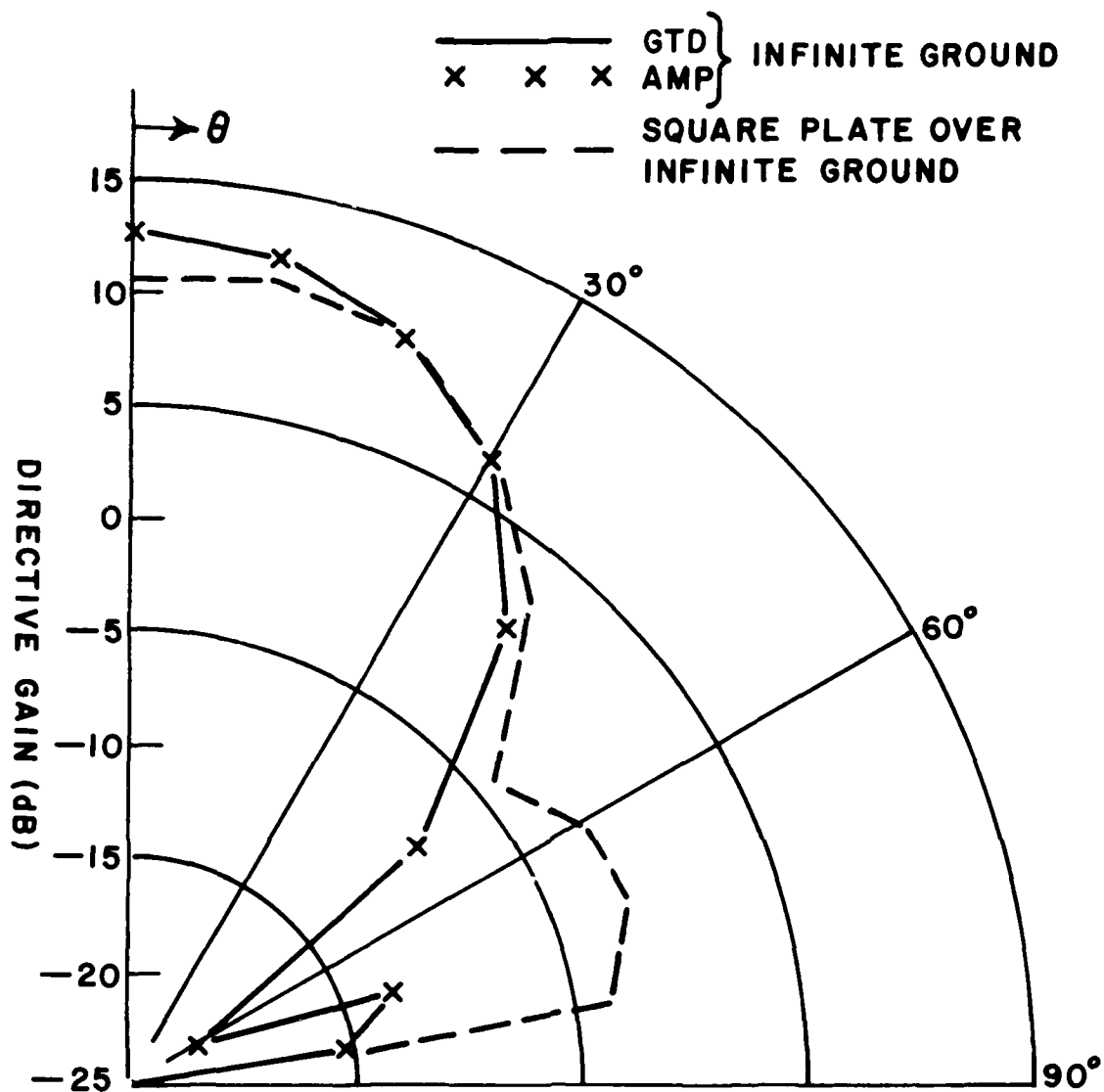


Figure 5a. Comparison of the total directive gain of four sets of crossed dipoles over an infinite ground and over a square plate over an infinite ground ($\phi=0^\circ$).

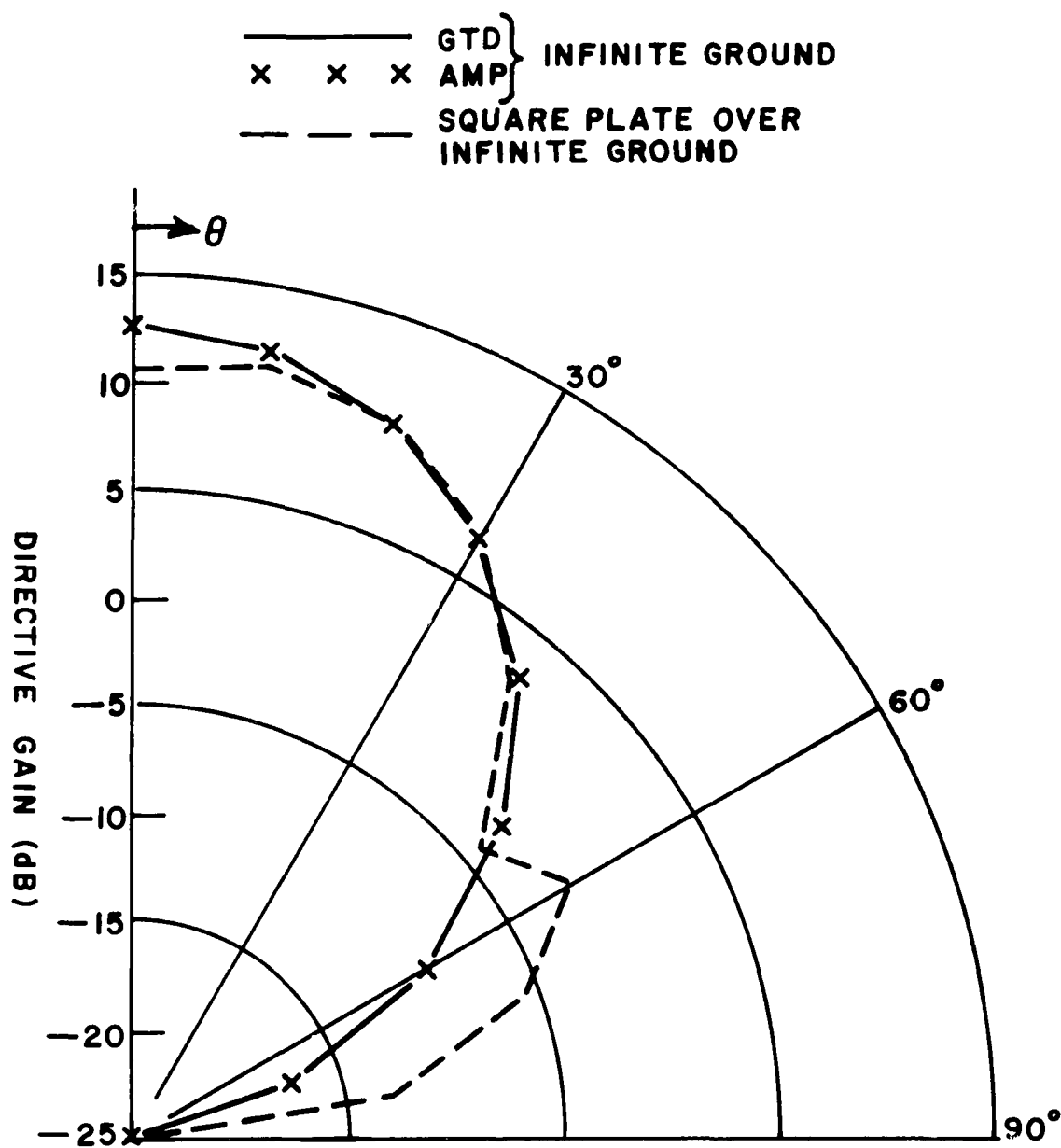


Figure 5b. Comparison of the total directive gain of four sets of crossed dipoles over an infinite ground and over a square plate over an infinite ground ($\phi=45^\circ$).

but the one-half pi factor and improvements in the print out representation of the directive gain have been added since delivery. An option allowing a range in the far field to be specified has also been added. These updates can easily be implemented in the delivered code. The user's manual is also under preparation and should be completed early in December 1977. The user's manual will explain in detail the input parameters and output data of the code. Specific examples will illustrate the versatility of the code and will clarify many of the subtleties involved in using it to simulate scattering structures.

IV. REFLECTOR ANTENNA CODE DEVELOPMENT

The major task of the present effort under the reflector antenna code development is to develop a user-oriented computer program package by which the far field pattern of a typical Navy reflector antenna can be calculated. Feed blockage and scattering effects are not included in this phase. These will be included later (see Table I).

The theoretical approach for computing the far field pattern of the general reflector is based on a combination of the Geometrical Theory of Diffraction (GTD) and Aperture Integration (AI) techniques. AI will be used to compute the main beam and near sidelobes; GTD will be used to compute the wide-angle sidelobes and the backlobes. To implement the computer algorithms based on these theories, efficient ways are being developed to handle calculations involving the feed pattern and the reflector geometry. The geometry of the reflector rim is treated as piece-wise linear.

Since the majority of Navy reflector antennas have parabolic surfaces, only the class of parabolic surfaces will be implemented in the computer code. The code for the reflector geometry will be flexible enough to include off-set fed reflectors and general reflector rim shapes such as elliptical and rectangular with chopped corners.

An efficient way to handle AI is necessary because of its time-consuming nature for electrically large reflectors. Fortunately, AI is needed only for the main beam and near sidelobe regions of the pattern. GTD is very efficient for calculating most of the pattern. Two techniques are being implemented to provide efficient AI: the polynomial-fit method for the feed pattern and the rotating grid method for the numerical integration required to calculate the far field pattern.

A. Feed Pattern

The polynomial-fit method is used to obtain an analytic fit for each measured pattern cut of the volumetric feed pattern. This method provides a computationally efficient way of calculating the aperture field without requiring large amounts of computer storage for the measured feed pattern. Only relatively few coefficients need to be stored for essentially complete feed pattern information. Furthermore, the

polynomial-fit method has the advantages of flexibility and simplicity for general feed patterns. No cut-and-try procedures are needed; the polynomial coefficients can be computed automatically from the measured feed pattern input.

Further improvement has been made for fitting measured feed patterns in the spillover region, i.e., where the feed radiation is not reflected by the reflector. At the low field levels encountered in the spillover region, a piecewise linear approximation was found to be a better representation for this part of the feed pattern. Thus the computer sub-routines were modified to use a combination of polynomial-fit for the major part of the feed pattern and a piecewise linear fit for most of the spillover region of the pattern.

Several subroutines have been developed to treat a feed with a general pattern and general polarization. These subroutines decompose the feed radiation into components to provide the necessary information for the following: 1) aperture fields, 2) GTD edge illuminations, and 3) direct feed radiation.

In the computer code the measured feed pattern is inputted at the angles $\phi = \phi_n$, $n=1,2,\dots,N_\phi$. The theory for obtaining the combined polynomial-linear fit for a specific input feed pattern cut at ϕ_n is given in the Annual Report [1]. The feed pattern in planes other than those corresponding to the input pattern cuts is calculated by linear interpolation. As a first step the nearest input pattern angles ϕ_Q and ϕ_P are determined for the desired feed pattern angle ϕ as shown in Figure 6. Then the pattern is calculated from

$$f(\psi, \phi') = Q_{DP} f(\psi, \phi_P) + (1-Q_{DP}) f(\psi, \phi_Q) \quad (1)$$

where

$$Q_{DP} = \frac{\phi - \phi_Q}{\phi_P - \phi_Q} \quad (2)$$

Various states of feed polarizations can be treated by using two orthogonal linear polarizations. The two linear polarization components are treated as those corresponding to dipoles oriented along the x-axis and the y-axis, respectively. Thus the electric field of the feed is given by

$$\vec{E}^f = [-\hat{\theta}_x A_x f_x(\psi, \phi') - \hat{\theta}_y A_y f_y(\psi, \phi')] \frac{e^{-jkR'}}{R'} \quad (3)$$

where $-\hat{\theta}_x$ and $-\hat{\theta}_y$ are the unit vectors corresponding to the respective dipole polarizations. The modified spherical coordinate system (R', ψ, ϕ')

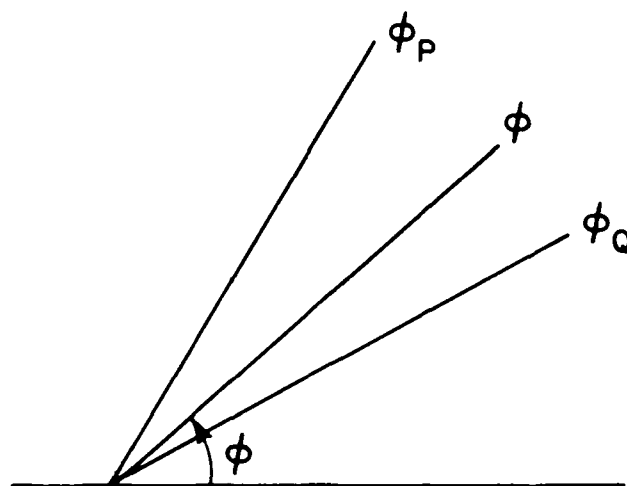


Figure 6. Interpolation of the feed pattern in the ϕ -plane.

for the feed pattern is shown in Figure 7a. The unit vector $\hat{\theta}_y$ is defined by the polar angle θ_y which is measured from the y-axis as shown in Figure 7b. The unit vector $\hat{\theta}_x$ is defined by the angle θ_x which is measured in the same way but from the x-axis.

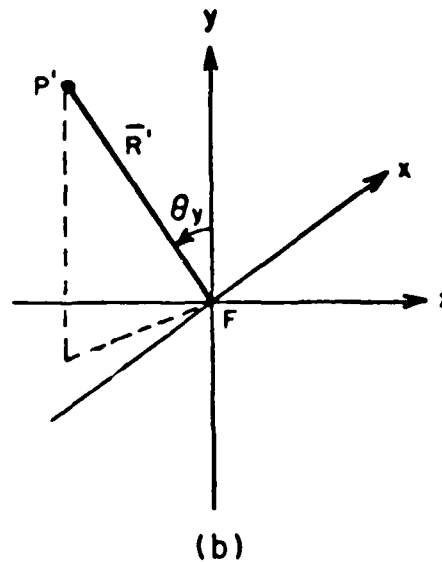
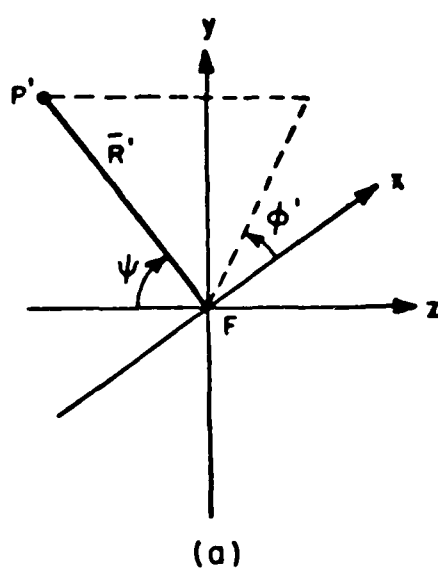


Figure 7. Coordinate systems for the primary feed.

Each pattern component f_x and f_y must be consistent for the direction $\psi=0$; thus $f_x(0, \phi')$ and $f_y(0, \phi')$ must be constant for all values ϕ' . The feed polarization is controlled by the complex constants A_x and A_y . For example, circular polarization can be obtained by setting $A_y = \pm j A_x$.

The unit vector $\hat{\theta}_x$ can be expressed in terms of $\hat{\theta}$ and $\hat{\phi}$ components of the standard spherical coordinate system (R, θ, ϕ) :

$$\begin{aligned}\hat{\theta} &= \frac{1}{B_x} [-\hat{\theta} \cos \theta \cos \phi + \hat{\phi} \sin \phi] \\ &= \frac{1}{B_x} [\hat{\theta} \cos \psi \cos \phi' + \hat{\phi} \sin \phi']\end{aligned}\quad (4)$$

where $\psi = \pi - \theta$ and $\phi' = \phi$ are the coordinate angles for the feed pattern and

$$B_x = \sqrt{1 - \sin^2 \psi \cos^2 \phi'} \quad (5)$$

Similarly the unit vector $\hat{\theta}_y$ is given by

$$\hat{\theta}_y = \frac{1}{B_y} [\hat{\theta} \cos \psi \sin \phi' - \hat{\phi} \cos \phi'] \quad (6)$$

where

$$B_y = \sqrt{1 - \sin^2 \psi \sin^2 \phi'} \quad (7)$$

Thus the feed pattern can be expressed as

$$\vec{E}^f = - [\hat{\theta} f_{\theta} + \hat{\phi} f_{\phi}] \frac{e^{-jkR'}}{R'} \quad (8)$$

where

$$f_{\theta} = \cos \psi \cos \phi' \frac{A_x}{B_x} f_x(\psi, \phi') + \cos \psi \sin \phi' \frac{A_y}{B_y} f_y(\psi, \phi') \quad (9)$$

and

$$f_{\phi} = \sin \phi' \frac{A_x}{B_x} f_x(\psi, \phi') - \cos \phi' \frac{A_y}{B_y} f_y(\psi, \phi') \quad (10)$$

Equation (8) is used to calculate the feed pattern for the direct feed radiation and also to determine the aperture field. For a paraboloidal surface with a feed at the focus the aperture field at point $P(x,y,z)$ as shown in Figure 8 is given by

$$E_x^a = - [\cos\phi' f_\theta(\psi, \phi') + \sin\phi' f_\phi(\psi, \phi')] \frac{e^{-jkR_0}}{R'} \quad (11)$$

and

$$E_y^a = - [\sin\phi' f_\theta(\psi, \phi') - \cos\phi' f_\phi(\psi, \phi')] \frac{e^{-jkR_0}}{R'} \quad (12)$$

The necessary coordinate information for the aperture field is defined by the point of reflection on the reflector surface with coordinates x, y as shown in Figure 8. Thus

$$R' = \sqrt{\rho^2 + z_p^2} \quad (13)$$

$$z_p = F - \frac{\rho^2}{4F} \quad (14)$$

$$\psi = \tan^{-1} \frac{\rho}{z_p} \quad (15)$$

and

$$\phi' = \tan^{-1} \frac{y}{x} \quad (16)$$

R_0 is the pathlength from the focus to the aperture plane which is defined as the plane perpendicular to the z -axis and passing through the reference point $P_0(x_0, y_0, z_0)$ on the reflector rim. Thus

$$R_0 = \sqrt{\rho_0^2 + z_0^2} \quad (17)$$

$$\rho_0 = \sqrt{x_0^2 + y_0^2} \quad (18)$$

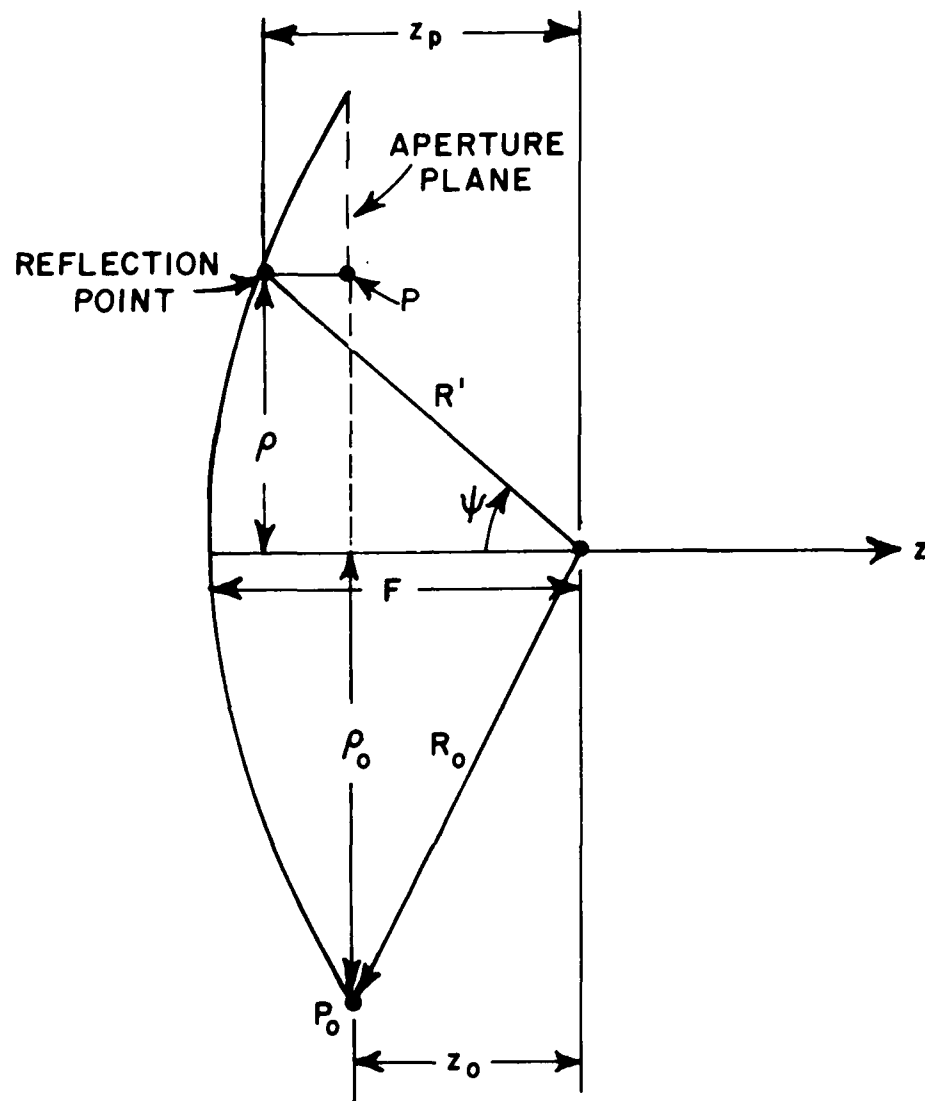


Figure 8. Coordinate system for the aperture field.

$$z_0 = F - \frac{\rho_0^2}{4F} \quad (19)$$

The field of the feed incident on the reflector rim is needed to calculate the diffracted field using the GTD approach. For this purpose it is convenient to decompose the feed polarization vectors $\hat{\theta}_x$ and $\hat{\theta}_y$ into rectangular components. Thus

$$\hat{\theta}_x = -\hat{x} B_x + \hat{y} \frac{\sin^2 \psi \cos \phi' \sin \phi'}{B_x} - \hat{z} \frac{\sin \psi \cos \psi \cos \phi'}{B_x} \quad (20)$$

and

$$\hat{\theta}_y = \hat{x} \frac{\sin^2 \psi \cos \phi' \sin \phi'}{B_y} - \hat{y} B_y - \hat{z} \frac{\sin \psi \cos \psi \sin \phi'}{B_y} \quad (21)$$

where B_x and B_y are given by Equations (5) and (7). Thus the field of the feed is expressed in rectangular components by

$$E_x^i = \left[-B_x A_x f_x(\psi, \phi') + \sin^2 \psi \cos \phi' \sin \phi' \frac{A_y}{B_y} f_y(\psi, \phi') \right] \frac{e^{-jkR'}}{R'} \quad (22)$$

$$E_y^i = \left[\sin^2 \psi \cos \phi' \sin \phi' \frac{A_x}{B_x} f_x(\psi, \phi') - B_y A_y f_y(\psi, \phi') \right] \frac{e^{-jkR'}}{R'} \quad (23)$$

and

$$E_z^i = -\sin \psi \cos \psi \left[\cos \phi' \frac{A_x}{B_x} f_x(\psi, \phi') + \sin \phi' \frac{A_y}{B_y} f_y(\psi, \phi') \right] \frac{e^{-jkR'}}{R'} \quad (24)$$

B. Rotating Grid Method

The rotating grid provides greatly improved efficiency for the far field pattern computations. With this approach the y-integration is carried out for each column of the aperture and each one-dimensional integration result is stored. The stored values for the y-integration are then used for each pattern angle θ in the plane perpendicular to the y-axis; thus the efficiency approaches that of a one-dimensional integration. Even though the integration grid must be rotated to obtain the pattern in other planes, the required grid rotation is computationally much faster than the numerous two-dimensional integrations that would otherwise be required. The computer algorithms for the rotating grid method have been developed and the method has been programmed on the OSU Datacraft computer.

Some typical far field pattern results from the rotating grid method were shown in the Annual Report [1]. The accuracy of these results were checked by using the rectangular subaperture method described in the Third Quarterly Report [2]. It was found that very accurate results could be achieved with very good computational efficiency. The rotating grid method was found to run 7-10 times faster than the rectangular subaperture method as shown in Table III.

C. GTD Method

The GTD will be used to calculate the wide-angle sidelobe and back-lobe regions for the reflector antenna computer code. Work is continuing on the development of the GTD portion of this code. Advantage is being taken of the existing GTD computer subroutines for the edge diffraction functions and the corner diffraction functions.

Part of the geometry subroutine from the flat plate scattering code has been modified for use in the GTD portion of the reflector antenna code. The 3-D geometry of the reflector rim is determined from the intersection of the projected rim shape and the parabolic reflector surface. The projected rim shape is specified as piece-wise linear as shown in Figure 9. The input for the rim geometry is specified by the X and Y coordinates of each junction point on the rim. The Z coordinate of each junction is given by

$$Z = \frac{x^2 + y^2 - \rho_0^2}{4F} \quad (25)$$

where F is the focal length of the parabola and ρ_0 is the radius to the reference point P_0 which defines the aperture plane and is given by Equation (18).

The geometry associated with the reflector rim is calculated and stored for use in calculating all of the diffracted fields via the GTD. The following information for the geometry is stored for each linear segment of the reflector rim:

- 1) the edge unit vectors,
- 2) the unit vector normal to the parabolic surface,
- 3) the unit binormal vector (perpendicular to the edge and normal vectors), and
- 4) the bounds on the permissible range for the diffraction angle.

COMPUTATION TIMES FOR REFLECTOR
ANTENNA PATTERNS
(CPU TIMES FOR AI ONLY IN SECONDS)

PATTERN PLANE	RECTANGULAR SUBAPERTURE	ROTATING GRID
------------------	----------------------------	------------------

$\phi = 0^\circ$	64.6	9.2	$19\lambda \times 11\lambda$ APERTURE WITH CHOPPED CORNERS $D_x = D_y = 0.5\lambda$ $\theta = 0(0.2^\circ)30^\circ$
$\phi = 30^\circ$	75.4	9.9	
$\phi = 45^\circ$	75.6	11.4	
	29 MIN.	4 MIN.	APPROXIMATE TIME TO COMPUTE $\phi = 0(15^\circ)345^\circ$

$\phi = 0^\circ$	57.3	5.0	$100\lambda \times 100\lambda$ SQUARE APERTURE $D_x = D_y = 2.5\lambda$ $\theta = 0(0.04^\circ)3^\circ$
$\phi = 30^\circ$	68.4	7.0	
$\phi = 45^\circ$	69.7	6.7	
	26 MIN.	$2\frac{1}{2}$ MIN.	APPROXIMATE TIME TO COMPUTE $\phi = 0(15^\circ)345^\circ$

TABLE III

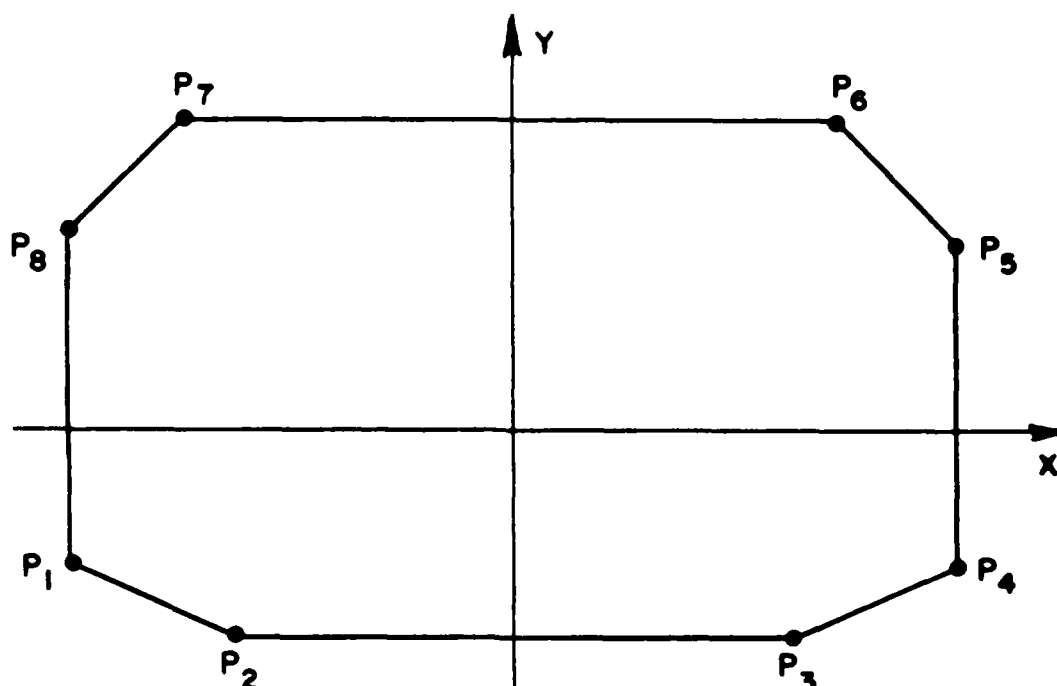


Figure 9. Reflector rim geometry.

In order to improve the computational efficiency of the code a shadow boundary subroutine has been developed to calculate the angles at which the shadow boundaries occur in the plane in which the pattern is calculated. Thus the subroutine will determine the pattern angles for which the direct feed pattern (feed spillover) must be included before the pattern is computed. This will eliminate the need to check whether the source or feed must be included for each pattern angle, as must be done in scattering codes with more than one scatterer.

When the GTD method is used the reflector code will increment around the rim and determine whether a diffraction occurs for each linear rim segment. This will be done by comparing the diffraction angle with the bounds on the permissible range of angles. If no diffraction occurs for that segment the code will check the next rim segment. If a diffraction does occur, the diffraction point and the vector for the incident ray from the feed will be calculated. This procedure is the same as that used for the flat plate scattering code except that the geometry information associated with the parabolic reflector surface is changed.

The incident field at the diffraction point is calculated from the feed pattern subroutines discussed in a previous section. The incident field is decomposed into rectangular components by use of Equations (22) through (24). The code then calculates the components

of the incident field perpendicular and parallel to the rim segment. The edge diffraction coefficients and the corner diffraction coefficients for the respective perpendicular and parallel components are calculated in the same way as for the flat plate. See Reference [3]. Finally the diffracted fields are calculated and summed for each rim segment.

Results have been obtained from the preliminary GTD code and it was found that the reflector rim must be subdivided into many straight line segments because of its 3-D curvature. This is true even though the projected rim shape may be composed of only a few straight line segments, e.g., the rectangular aperture. A criterion for subdividing the reflector rim is currently being checked.

V. THEORETICAL STUDIES

The completion date for the slope diffraction report has been changed to 31 January 1978. This delay has been caused by a shift of emphasis to the work on double diffraction which was being carried out by Professor Tiberio, a visiting professor from the University of Florence, Italy. Professor Tiberio has been forced to return to Italy sooner than expected and Professor Kouyoumjian had to drop the slope diffraction work in order to help Professor Tiberio complete his phase of the double diffraction work. It is anticipated that the preparation of the report on slope diffraction will be resumed in November or by December at the latest and completed by 31 January 1978.

REFERENCES

1. Burnside, W.D., R.G. Kouyoumjian, R.J. Marhefka, R.C. Rudduck and C.H. Walter, "Asymptotic High Frequency Techniques for UHF and Above Antennas," Annual Report 4508-6, August 1977, The Ohio State ElectroScience Laboratory, Department of Electrical Engineering; prepared under Contract N00123-76-C-1371 for Naval Regional Procurement Office.
2. Burnside, W.D., R.G. Kouyoumjian, R.J. Marhefka, R.C. Rudduck and C.H. Walter, "Asymptotic High Frequency Techniques for UHF and Above Antennas," Third Quarterly Report 4508-5, May 1977, The Ohio State University ElectroScience Laboratory, Department of Electrical Engineering; prepared under Contract N00123-76-C-1371 for Naval Regional Procurement Office.
3. Marhefka, R.J., "Analysis of Aircraft Wing-Mounted Antenna Patterns," Report 2902-25, June 1976, The Ohio State University ElectroScience Laboratory, Department of Electrical Engineering; prepared under Grant NGL 36-008-138 for National Aeronautics and Space Administration.

END

FILMED

9-83

DTIC